JACS
JOURNAL OF THE AMERICAN CHEMICAL SOCIETY

Article

pubs.acs.org/JACS

Disease Detection by Ultrasensitive Quantification of Microdosed Synthetic Urinary Biomarkers

Andrew D. Warren,[†,‡] Shonda T. Gaylord,[§,‡] Kevin C. Ngan,[§] Milena Dumont Milutinovic,[§] Gabriel A. Kwong,[†] Sangeeta N. Bhatia,*[,†] and David R. Walt*[,§]

[†]Harvard-MIT Division of Health Sciences and Technology, Massachusetts Institute of Technology, 77 Massachusetts Avenue, Building 76-453, Cambridge, Massachusetts 02139, United States

[§]Department of Chemistry, Tufts University, 62 Talbot Avenue, Medford, Massachusetts 02155, United States

Supporting Information

ABSTRACT: The delivery of exogenous agents can enable noninvasive disease monitoring, but existing low-dose approaches require complex infrastructure. In this paper, we describe a microdose-scale injectable formulation of nanoparticles that interrogate the activity of thrombin, a key regulator of clotting, and produce urinary reporters of disease state. We establish a customized single molecule detection assay that enables urinary discrimination of thromboembolic disease in mice using doses of the nanoparticulate diagnostic agents that fall under regulatory guidelines for "microdosing."

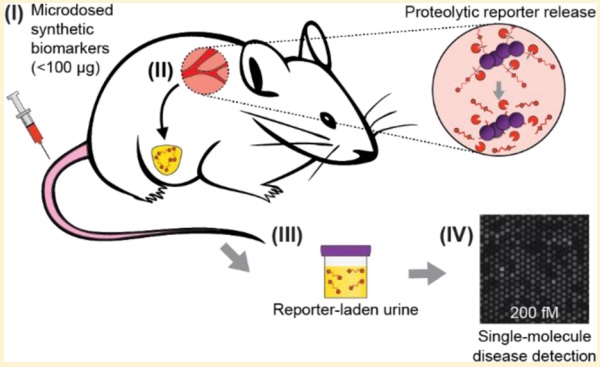

1. INTRODUCTION

Biomarkers are endogenously produced indicators of biological state and encompass metabolites, proteins, nucleic acids, and other biological compounds.[1] An ideal biomarker provides specific information about a disease for screening, diagnosis, or prognosis. Unfortunately, biomarkers are often limited by lack of specificity or sensitivity, interpatient variability, or poorly understood disease-biomarker biology.[2] A promising strategy to bypass these limitations is to introduce exogenous compounds that exploit pathological differences in metabolism, biodistribution, or excretion to produce a unique, specific, and detectable biomarker. An example is [^{18}F]fluoro-2-deoxyglucose, which is metabolized identically to glucose and enables visualization of diseases with increased glucose metabolism (e.g., cancer, Alzheimer's disease) by positron emission tomography (PET).[3]

In a similar vein, we have developed "synthetic biomarkers", nanoparticle agents that sample disease-associated proteases and produce a urinary signal.[4−6] Upon intravenous (IV) injection, synthetic biomarkers passively home to sites of disease, where reporters are liberated by proteolytic cleavage of a disease-tuned peptide substrate and subsequently filter into the urine as reporters of disease state (Figure 1A). Although synthetic biomarkers have the potential to improve disease diagnosis and monitoring, a challenge to their adoption is the use of administered synthetic compounds, which require rigorous evaluation by the U.S. Food and Drug Administration (FDA) before approval and use in humans. By comparison, the FDA approval time frame for new radioisotope agents can be minimized by using minute doses that are still detectable owing to PET's remarkable sensitivity and are therefore regulated as "microdoses" (≤100 μg), greatly compressing the time frame and simplifying the translational path to the clinic.[7]

Inspired by this approach, we combined our existing single molecule array (SiMoA) technology with synthetic biomarkers to enable disease detection at microdose levels. SiMoA technology has been applied to the subfemtomolar detection of PSA, HIV p24 protein, genomic DNA and cytokines based on counting of single molecules.[8,9] SiMoA uses antibody-coated capture beads to facilitate the formation of enzyme-labeled sandwich complexes in the presence of low concentrations of analyte; upon singulation of beads into ∼50 000 50 fL fiber optic wells, the signal generated by fluorogenic substrate cleavage from even a single enzyme-labeled sandwich complex may be detected. Using reformulated disease reporters with stable poly(ethylene glycol) linkers, we modified the SiMoA technology to capture and directly detect synthetic compounds rather than biologically derived molecules without relying on a sandwich immunoassay by using prebiotinylated analytes that reduce processing time, reagent use, and sources of noise introduced by secondary recognition agents.

These new tools allow study of stability, pharmacokinetics, and diagnostic performance at microdose levels, without requiring use of radioactive or stable isotope reformulations of our reporters as required in previous types of microdose

Received: June 5, 2014
Published: September 8, 2014

dx.doi.org/10.1021/ja505676h | J. Am. Chem. Soc. 2014, 136, 13709−13714

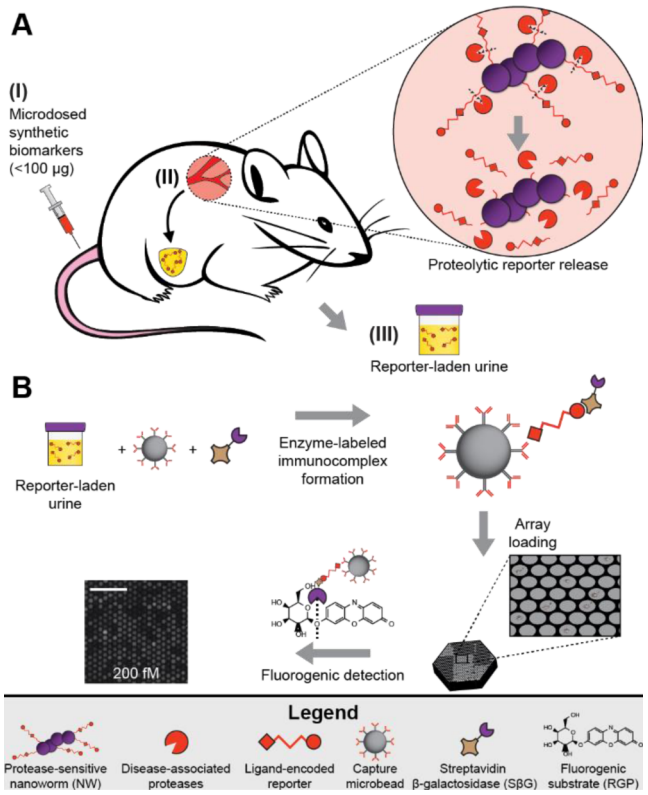

Figure 1. (A) Injected synthetic biomarkers (I) release reporters upon interaction with disease-associated proteases (II). Ligand-encoded reporters liberated from carrier nanoparticles are small enough to be concentrated into the urine (III). (B) The SiMoA assay uses capture antibody-coated beads and SβG to form reporter–sandwich complexes. Beads are loaded into arrays of ~50 000 wells and sealed with fluorogenic substrate RGP to detect single sandwich complexes. Scale is 50 μm.

studies.[3,7] Here, we describe the use of microdosed thrombin-sensitive synthetic biomarkers in mice coupled to our customized single molecule detection platform (Figure 1B) to detect thrombosis, a disease with poor biomarkers owing to an inability to directly detect thrombin activity and a reliance on measuring upstream or downstream byproducts of clotting.[5,10] Our approach obviates costly, specialized radioisotopes and sophisticated sample preparation typical of microdose studies.

2. EXPERIMENTAL SECTION

2.1. Reporter/Peptide Synthesis. Thrombin-sensitive peptides were synthesized by CPC Scientific, with the sequence Biotin-PEG_{5kDa}-Lys(5FAM)-Gly-Gly-DPhe-Pro-Arg-Ser-Gly-Gly-Gly-Cys, where PEG_{5kDa} is 5 kDa poly(ethylene glycol). Standard (nonprotease-sensitive) ligand-encoded reporters R1–2 were synthesized by derivatizing biotin-poly(ethylene glycol) 5 kDa-amine (Laysan) with NHS-fluorescein (R1; Sigma) or NHS-Alexa Fluor 488 (R2; Invitrogen).

2.2. Protease-Sensitive R1-Nanoworm (NW) Synthesis. Dextran-cross-linked nanoworms (NWs) were synthesized as previously described.[11,12] Aminated NWs were activated with *N*-succinimidyl iodoacetate (SIA; Pierce) in a 500-fold molar excess to NWs. Activated NWs were purified and reacted with sulfhydryl-terminated protease-sensitive peptide reporters (95-fold excess; thrombin-sensitive R1 is terminated with a cysteine) and $mPEG20_kDa$-SH (20-fold excess) for 1 h, resulting in thrombin-sensitive peptide valency of 50–70 per NW. R1-NW concentrations refer to the concentration of thrombin-sensitive R1-substrate peptides on the NW surface, with molecular weight of NW carrier included (see Supporting Information for calculations).

2.3. Enzyme-Linked Immunosorbent Assay (ELISA). ELISAs for modified R1–2 were performed as previously described.[5,6] Briefly, fluorescein antibody (αR1; Genetex) or Alexa Fluor 488 antibody (αR2; Life Technologies) were adsorbed to 96-well Bacti plates (Thermo Scientific) at 0.4–0.8 μg/mL. Following washing with PBS with 0.05% (v/v) Tween 20, plates were blocked with PBS with 1% (w/v) bovine serum albumin (BSA; Sigma). Urine samples (diluted $1:10^2$–10^4) and R1–2 standards were applied. Following washing, antibody–reporter–neutravidin sandwich complexes were formed by the addition of 0.4 μg/mL NeutrAvidin-horseradish peroxidase (Pierce). Sandwich complexes were detected by the oxidation of chromogenic substrate 3,3′,5,5′-tetramethylbenzidine (Pierce) at 450 nm and reporter concentration was calculated using the linear response region of reporter standards.

2.4. Single Molecule Array (SiMoA) Assay. Carboxylic acid functionalized paramagnetic beads (2.7 μm, Agilent Technologies) were covalently coupled with capture antibody (same as for ELISA) via 1-ethyl-3-(3-(dimethylamino)propyl)carbodiimide hydrochloride (EDC; Thermo Scientific) coupling protocol. Antibody-functionalized beads were blocked with PBS with 1% (w/v) BSA and roughly 200 000 beads were incubated with reporter standards or urine (diluted 10^2–10^4). Following addition of streptavidin-β-galactosidase to complete the sandwich complex, fiber optic arrays with 50 000 chemically etched wells were loaded with washed beads by centrifugation. Individual wells were sealed with fluorescent substrate resorufin-β-D-galactopyranoside (RDG; Life Technologies) and local fluorescence generated by substrate cleavage was imaged by custom equipment.[9]

2.5. Enzyme Kinetics. Michaelis–Menten enzyme kinetics were observed using an intramolecularly quenched reporter with the structure 5FAM-Gly-Gly-DPhe-Pro-Arg-Ser-Gly-Gly-Gly-Lys(CPQ2)-Lys-PEG_2-Cys (CPC Scientific), which fluoresces upon proteolytic substrate cleavage. Intramolecularly quenched reporter was incubated with recombinant thrombin (2 nM, Haematologic Technologies) and substrate cleavage velocity was observed via fluorimeter. To quantify release kinetics of R1 from thrombin-sensitive R1-NWs, we added physiologic levels of recombinant thrombin (15 nM),[13] purified released reporters by filtration (30 kDa M_r Amicon Ultra filters; Millipore), and quantified proteolytically released reporters by ELISA or SiMoA.

2.6. R1 Renal Clearance. MIT's committee on animal care approved all animal studies (protocol 0411-036-14), which were performed with 6–10 week female Swiss Webster mice (Taconic). Excretion dose–response experiments were performed by intravenous injection of free R1 (not protease-sensitive, in 200 μL of PBS, $n = 3$ mice) followed by collection of all urine from 0 to 60 min postinjection. Log–log linear fit was performed using average urine concentration from $n = 3$ mice at five injected doses. Urine was weighed to calculate volume and frozen at −80 °C until analysis by ELISA (200–20 000 fmol) or SiMoA (0.2–20 fmol). Urinary recovery was calculated as total reporter excreted (the product of urine concentration with urine volume) normalized to injected dose.

2.7. Disease Detection with R1-NWs and R2. Thrombin-sensitive R1-NWs and renal clearance control R2 were intravenously (IV) co-injected in equimolar amounts at 0.2–200 pmol in 200 μL of PBS into female Swiss Webster mice ($n = 5$–10 per concentration) and all urine 0–30 min postinjection was collected to obtain control clearance values. A total of 3–5 days later (to allow synthetic biomarker clearance), mice were again co-injected with R1-NWs and R2 along with 20 U/g thromboplastin (Biopharm Laboratories) to induce intravascular coagulation as previously described[5,14] and all urine 0–30 min postinjection was collected and pooled. R1 and R2 concentration was quantified by ELISA (20–200 pmol) or SiMoA (0.2–2 pmol).

dx.doi.org/10.1021/ja505676h | J. Am. Chem. Soc. 2014, 136, 13709–13714

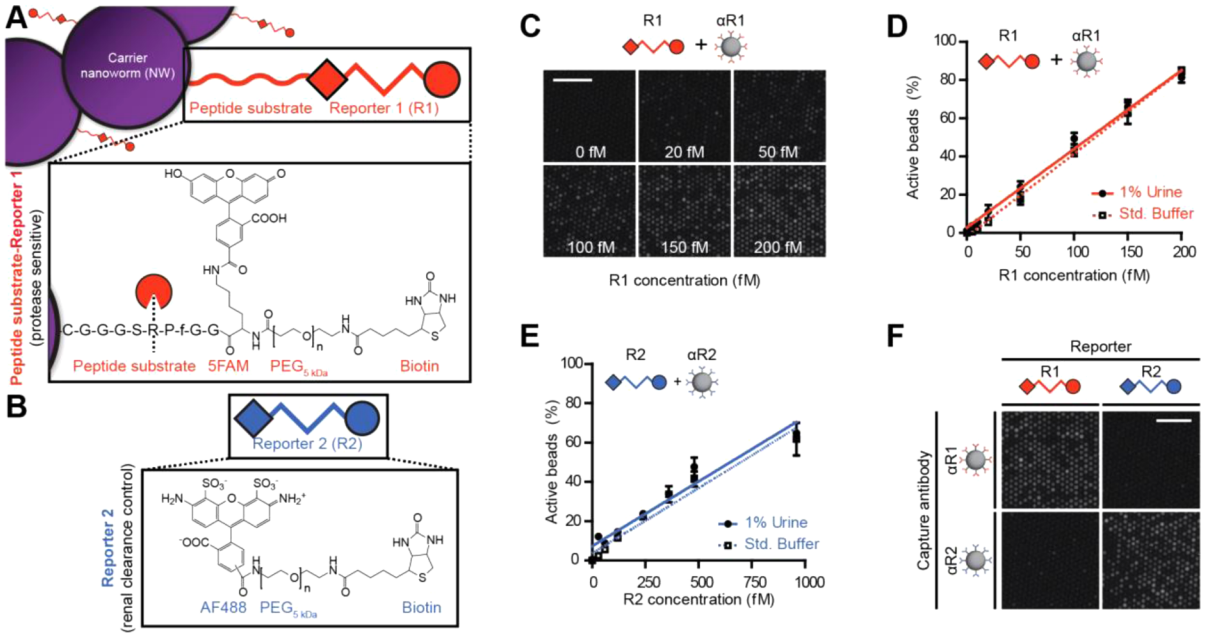

Figure 2. (A) Protease-sensitive synthetic biomarkers release reporter 1 (R1; structure fluorescein-PEG$_{5kDa}$-Biotin) from carrier NWs upon proteolytic cleavage of thrombin substrate. (B) Renal clearance control R2 is protease insensitive and uses Alexa Fluor 488 as capture ligand. (C) SiMoA assay with αR1-coated beads and increasing concentrations of R1 resulted in higher proportions of active fluorescent wells. (D) SiMoA assay for R1 demonstrated a linear relationship between active beads and R1 concentration from 5 to 200 fM and was unaffected by incubation with 1% control mouse urine. (E) The R2 SiMoA assay resulted in a similar linear relationship from 50 to 1000 fM. (F) Combination of R1 or R2 with αR1- or αR2-coated beads results in signal only from appropriately paired reporters and capture antibodies. Scale bar is 50 μm.

3. RESULTS AND DISCUSSION

3.1. Synthetic Biomarker Design. Our thrombin-sensitive synthetic biomarkers consist of iron oxide nanoworms (NWs) decorated with reporters bound to the NW surface by proteolytically degradable peptide substrates. Extensively characterized as biocompatible and long-circulating, the NWs are synthesized by the reaction of Fe(II) and Fe(III) salts in the presence of dextran[11,12] and serve as carriers that render urinary reporter accumulation contingent upon thrombin-mediated degradation of the linking peptide substrate. To enable femtomolar-scale detection from the urine via sandwich complex assay, we designed our ligand-encoded reporter R1 with a capture ligand (fluorescein; for reporter immobilization), a detection ligand (biotin; for enzyme-mediated amplification), and a nondegradable poly(ethylene glycol) (PEG) 5 kDa spacer to enable favorable pharmacokinetics and simultaneous binding of both ligands (Figure 2A). The use of biotin enables direct detection of captured reporters without needing to form sandwich immunocomplexes, thus simplifying the assay. To account for differences in renal clearance, we designed a second orthogonal reporter R2, which passively filters into the urine and is not protease sensitive, with the structure Alexa Fluor 488-PEG$_{5kDa}$-biotin (Figure 2B).

3.2. ELISA and SiMoA Assay. By conventional ELISA, the reporters are detected at low picomolar concentrations.[5,6] For ultrasensitive reporter quantification, we modified our existing single molecule array technology, which relies on reporter capture by antibody-coated beads.[8,9] In the digital sandwich assay approach used here, capture beads are incubated with analyte and, subsequently, with streptavidin β-galactosidase (SβG) as an enzyme label that enables direct detection of bead-bound reporters. At very low analyte concentrations where many more beads are present than analyte molecules, the distribution of sandwich complexes may be described by Poisson statistics and is linearly proportional to concentration (Supporting Information Figures S1A and B). Beads are then loaded by centrifugation into an array of ~50 000 chemically etched wells, incubated with fluorogenic substrate resorufin-β-D-galactopyranoside (RGP), and sealed in individual 50 fL wells where a single enzyme label can generate detectable fluorescence.

SiMoA assay using αR1-coated beads resulted in an increase of fluorescent wells proportional to R1 concentration (Figure 2C). Quantitative imaging demonstrated a linear relationship between R1 concentration and active wells over a range of 5–200 fM that was unaffected by 1% control mouse urine; similar results were obtained with the R2 assay (Figures 2D,E; R2 linear range 50–1000 fM). To confirm R1–2 assay specificity, we applied saturating concentrations of each reporter to capture beads containing the other capture agent (e.g., R1 with αR2 and vice versa), resulting in no detectable off-target binding (Figures 2F, Supporting Information Figure S1C). These initial results indicated that the SiMoA assays were nearly 1000× more sensitive than the corresponding ELISAs and demonstrate the versatility of SiMoA for the sensitive detection of rationally designed synthetic compounds.

3.3. Enzymatic Reporter Release and Renal Clearance Kinetics. It is important that enzymatic kinetics are sufficiently fast at low synthetic biomarker concentrations to enable microdosing to be useful. Furthermore, linear dose–response of reporter excretion is required for unbiased disease detection. Nonlinearities in metabolism or excretion are a common microdosing mode of failure, often due to low-capacity, high-affinity drug binding reservoirs or dose-dependent metabolism. To demonstrate susceptibility of our synthetic biomarkers to proteolytic cleavage, we incubated a fluorescent reporting variant of our thrombin-sensitive NWs with thrombin, demonstrating thrombin-mediated peptidolysis with K_m =

dx.doi.org/10.1021/ja505676h | J. Am. Chem. Soc. 2014, 136, 13709–13714

3.55 μM and V_{max} = 2.26 nM s^{-1} (Figure 3A; $[E]_0$ = 2 nM). Quasi-steady-state Michaelis–Menten enzyme kinetics approx-

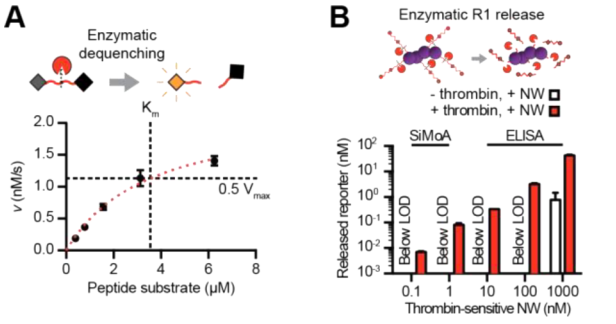

Figure 3. (A) In vitro incubation of a fluorescent reporter substrate with thrombin gave K_m = 3.55 μM and V_{max} = 2.26 nM s^{-1}. (B) Incubation of thrombin-sensitive NWs with thrombin resulted in an approximately linear relationship between released reporter concentration and input concentration.

imate enzymatic velocity (v) as linear with substrate concentration at low concentrations (for $[S] \ll K_m$, $v \approx V_{max}[S]/K_m$). Incubation of thrombin-sensitive NWs with physiological concentrations of thrombin ($[E]_0$ = 15 nM; catalytically active thrombin during clotting is typically ~10–30 nM)[13] at 37 °C for 60 min demonstrated approximately linear scaling of released reporter concentrations with NW concentration over four logs (Figure 3B).

To determine renal clearance efficiencies of our reporters, we quantified R1 concentration in urine excreted 0–60 min following IV injection of R1 and observed a linear relationship between injection and urine concentration (Figure 4A, log–log

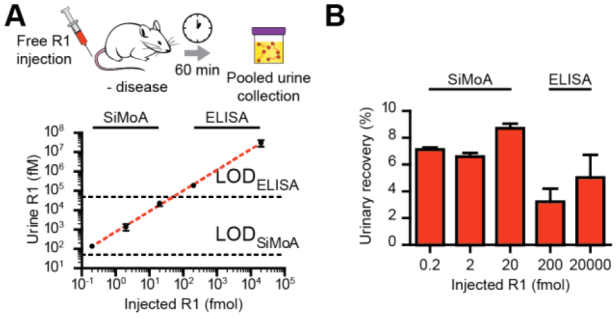

Figure 4. (A and B) IV injection of R1 and measurement of pooled urine concentration after 60 min demonstrated a linear dose–response relationship in urine concentration and no decrease in urine excretion percentage with decreasing dose.

linear fit of mean value R^2 = 1.00, n = 3 mice for each of five concentrations). To examine total reporter excretion, we compared urinary reporter recovery (total reporter excreted over total reporter injected) and found that percent excretion did not decrease over five logs of input dose (Figure 4B).

3.4. Disease Detection Using Microdoses of Synthetic Biomarkers. Favorable synthetic biomarker pharmacokinetics at low concentrations support the use of microdosed synthetic biomarkers to detect disease using an induced model of pulmonary embolism in mice. As demonstrated by our group and others in the hematology literature, IV administration of thromboplastin results in the formation of blood clots via the extrinsic clotting cascade that embolize to the lungs to recapitulate this life-threatening condition.[5,14,15]

Previous studies by our group used 0.2–1.0 nmol of injected NWs to detect disease;[4–6] here, we examined the ability of our reformulated synthetic biomarkers dosed at 200, 20, 2, and 0.2 pmol (1–1000× lower amounts than previously demonstrated) to diagnose thrombosis in vivo when paired with our new SiMoA assay. As anticipated, dosage of thrombin-sensitive R1-NWs and renal clearance control R2 at 200 pmol demonstrated greater R1 urinary concentration in the presence of disease (P = 0.0027), with R2 remaining relatively unaffected (P = 0.30, Figure 5A). These trends were successfully recapitulated at 0.2

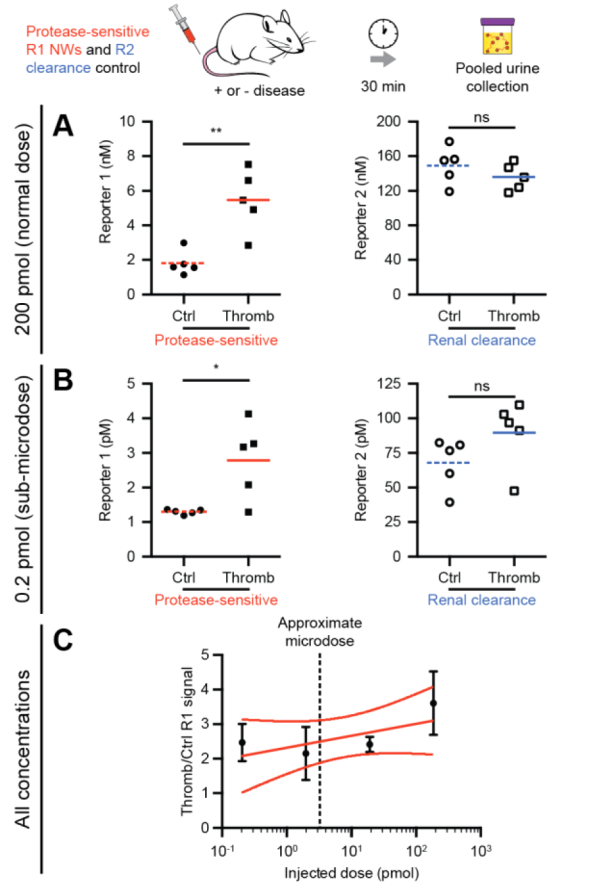

Figure 5. (A) Injection of 200 pmol thrombin-sensing R1-NWs and renal clearance control R2 demonstrated detection of disease by a significant increase in urine R1 concentration (P = 0.0027) but no significant change in control reporter R2 concentration (P = 0.30). (B) Injection of 1000-fold lower amounts of thrombin-sensing R1-NWs and control R2 demonstrated a significant increase in disease-sensitive R1 release (P = 0.017) but no significant change in control reporter R2 (P = 0.15). (C) Normalization of thrombin-sensitive R1-NW release in diseased mice to control mice revealed an average 2.35-fold increase in R1 signal over 3 orders of magnitude injected dose with a best fit line slope that did not deviate significantly from zero (P = 0.22).

pmol, 1000-fold lower and below microdose levels, demonstrating increased thrombin-sensitive R1 clearance (P = 0.017) in response to disease with urinary clearance control R2 remaining constant (P = 0.15, Figure 5B). On average, fold increase in urinary accumulation of R1 in response to clotting did not change with respect to concentration (slope of fit does not deviate significantly from zero with P = 0.22, Figure 5C). Collectively, these results indicate that our customized SiMoA assay could enable microdosed disease detection using synthetic biomarkers reformulated for low-dose applications.

dx.doi.org/10.1021/ja505676h | J. Am. Chem. Soc. 2014, 136, 13709–13714

4. CONCLUSION

In this paper, we described a custom single molecule assay that enables detection of synthetic ligand-encoded reporters. While previous SiMoA technologies have required sandwich immunocomplex formation for detection, we demonstrate femtomolar quantification of directly labeled targets that decreases processing time, reagent use, and obviates use of secondary recognition agents. When combined with a microdosed disease-tailored nanoparticle formulation, this modified SiMoA assay enables noninvasive urinary discrimination of thrombosis, a disease with poor existing biomarkers. Currently available diagnostics for thrombosis typically rely on sampling blood or urine for byproducts either upstream or downstream of the clotting cascade and efforts to directly detect thrombin activity rely on blood samples or do not provide a clinically useful urinary readout.[10,16,17]

Looking forward, our synthetic biomarker technology could be useful in conditions such as deep vein thrombosis (DVT) where the determination of clotting kinetics in stable vs extending thrombi would provide clinically actionable information. Others have shown the utility of thrombin-sensitive formulations in differentiating stable vs unstable atherosclerotic plaques, but these approaches have relied on fluorescent detection;[17] our platform could conceivably provide urinary monitoring without a need for imaging. Finally, the ability to detect disease with up to 1000× lower doses of synthetic biomarkers could facilitate the development of implants that slowly elute microdoses of protease sensors that enable near-continuous urinary monitoring of thrombotic events.

Previous efforts to diagnose disease using microdosed compounds typically rely on radiolabeled drugs and complex detection techniques like accelerator mass spectrometry (AMS) or PET;[18] here, we show radiolabel-free detection of rationally designed, proteolytically released fragments in urine using a single molecule-sensitive assay platform. In contrast to unstable radiolabels, the synthetic biomarker injectable is stable at 4 °C and the reporter-laden urine may be stored frozen long-term prior to analysis. Our platform enables detection sensitivities greater than traditional MALDI/MS or LC/ESI-MS/MS systems, while allowing rapid, multiplexed reporter detection and sensitivities roughly comparable to AMS without the need for time-consuming and difficult sample preparation.[19] Consequently, the synthetic and analytical infrastructures are greatly simplified compared to existing low dose strategies for disease diagnosis.

To successfully microdose synthetic biomarkers, scaling between mouse and human should be considered. Although interspecies protease kinetics are similar (Supporting Information Table S1), dosing disparities are due to blood volume (scales linearly with weight[20]) and renal filtration (slower in humans[21]). Here, the lowest functional synthetic biomarker dose was 0.2 pmol (3.9 ng). To maintain synthetic biomarker plasma concentration, the corresponding human dose is predicted to be ∼8.7 μg, well under the 100 μg microdose threshold (see Supporting Information). Interspecies differences in renal function (inulin's half-life is ∼16 times longer in humans than in mice) and the expected lower urine reporter concentrations may be resolved by the high sensitivity of the SiMoA.

The single molecule-sensitive SiMoA platform enables the use of multiplexable microdose-scale protease sensitive exogenous agents to detect disease, without the need for radiochemical synthesis, unstable reagents, or costly imaging platforms typical of microdose studies. These advances enable simplified, low cost (a single SiMoA assay is a few U.S. dollars), and safe diagnosis of thrombosis. Furthermore, they demonstrate the feasibility of more generalizable sandwich complex-based approaches to analysis that use the same diagnostics platform across broad concentration scales for different applications, from microdosing to standard clinical or point-of-care settings. By targeting different aberrantly regulated proteases with modified nanoparticles, the platform should be applicable to a broad variety of diseases including cancers, fibrosis, and inflammatory disorders.

■ ASSOCIATED CONTENT

Supporting Information

Text S1, giving detailed experimental protocols and calculations; Figure S1, expanding upon SiMoA assay validation; Figure S2, demonstrating first-order exponential clearance kinetics of urinary reporters; Figure S3, displaying all in vivo disease detection data; Table S1, comparing hemostatic coagulation indices between mouse and humans. This material is available free of charge via the Internet at http://pubs.acs.org.

■ AUTHOR INFORMATION

Corresponding Authors

sbhatia@mit.edu

David.Walt@tufts.edu

Author Contributions

‡A.D.W. and S.T.G. contributed equally.

Notes

The authors declare no competing financial interest.

■ ACKNOWLEDGMENTS

We thank Prof. D. Wood and Dr. H. Fleming for guidance. A.D.W. thanks the NSF Graduate Research Fellowship Program for support. G.A.K. acknowledges support from the Ruth L. Kirchstein NRSA (F32CA159496-02) and holds a Career Award at the Scientific Interface from the Burroughs Wellcome Fund. This work was supported in part by the Koch Institute Support (core) Grant P30-CA14051 from the National Cancer Institute as well as a grant from the Koch Institute Frontier Research Program through the Koch Institute Frontier Research Fund. S.N.B. is an HHMI investigator.

■ REFERENCES

(1) Hanash, S. M.; Pitteri, S. J.; Faca, V. M. *Nature* **2008**, *452* (7187), 571−9.

(2) Lutz, A. M.; Willmann, J. K.; Cochran, F. V.; Ray, P.; Gambhir, S. S. *PLoS Med.* **2008**, *5* (8), e170.

(3) Wagner, C. C.; Langer, O. *Adv. Drug Delivery Rev.* **2011**, *63* (7), 539−46.

(4) Kwong, G. A.; von Maltzahn, G.; Murugappan, G.; Abudayyeh, O.; Mo, S.; Papayannopoulos, I. A.; Sverdlov, D. Y.; Liu, S. B.; Warren, A. D.; Popov, Y.; Schuppan, D.; Bhatia, S. N. *Nat. Biotechnol.* **2013**, *31* (1), 63−70.

(5) Lin, K. Y.; Kwong, G. A.; Warren, A. D.; Wood, D. K.; Bhatia, S. N. *ACS Nano* **2013**, *7* (10), 9001−9.

(6) Warren, A. D.; Kwong, G. A.; Wood, D. K.; Lin, K. Y.; Bhatia, S. N. *Proc. Natl. Acad. Sci. U.S.A.* **2014**, *111* (10), 3671−6.

(7) Kummar, S.; Doroshow, J. H.; Tomaszewski, J. E.; Calvert, A. H.; Lobbezoo, M.; Giaccone, G.; Task Force on Methodology for the Development of Innovative Cancer Therapies (MDICT). *Eur. J. Cancer* **2009**, *45* (5), 741−6.

(8) Chang, L.; Song, L.; Fournier, D. R.; Kan, C. W.; Patel, P. P.; Ferrell, E. P.; Pink, B. A.; Minnehan, K. A.; Hanlon, D. W.; Duffy, D. C.; Wilson, D. H. *J. Virol. Methods* **2013**, *188* (1−2), 153−60.
(9) (a) Rissin, D. M.; Kan, C. W.; Campbell, T. G.; Howes, S. C.; Fournier, D. R.; Song, L.; Piech, T.; Patel, P. P.; Chang, L.; Rivnak, A. J.; Ferrell, E. P.; Randall, J. D.; Provuncher, G. K.; Walt, D. R.; Duffy, D. C. *Nat. Biotechnol.* **2010**, *28* (6), 595−9. (b) Rissin, D. M.; Fournier, D. R.; Piech, T.; Kan, C. W.; Campbell, T. G.; Song, L.; Chang, L.; Rivnak, A. J.; Patel, P. P.; Provuncher, G. K.; Ferrell, E. P.; Howes, S. C.; Pink, B. A.; Minnehan, K. A.; Wilson, D. H.; Duffy, D. C. *Anal. Chem.* **2011**, *83* (6), 2279−85.
(10) (a) Brill-Edwards, P.; Lee, A. *Thromb. Haemostasis* **1999**, *82* (2), 688−94. (b) Ginsberg, J. S.; Wells, P. S.; Kearon, C.; Anderson, D.; Crowther, M.; Weitz, J. I.; Bormanis, J.; Brill-Edwards, P.; Turpie, A. G.; MacKinnon, B.; Gent, M.; Hirsh, J. *Ann. Int. Med.* **1998**, *129* (12), 1006−11. (c) Bounameaux, H.; de Moerloose, P.; Perrier, A.; Reber, G. *Thromb. Haemostasis* **1994**, *71* (1), 1−6. (d) Kockum, C. *Thromb Res.* **1980**, *19* (4−5), 639−46. (e) Becker, R. C.; Spencer, F. A. *J. Thromb. Thrombolysis* **1998**, *5* (3), 215−229.
(11) Park, J. H.; von Maltzahn, G.; Zhang, L.; Schwartz, M. P.; Ruoslahti, E.; Bhatia, S. N.; Sailor, M. J. *Adv. Mater.* **2008**, *20* (9), 1630−5.
(12) Park, J. H.; von Maltzahn, G.; Zhang, L.; Derfus, A. M.; Simberg, D.; Harris, T. J.; Ruoslahti, E.; Bhatia, S. N.; Sailor, M. J. *Small* **2009**, *5* (6), 694−700.
(13) (a) Brummel, K. E.; Paradis, S. G.; Butenas, S.; Mann, K. G. *Blood* **2002**, *100* (1), 148−52. (b) Mann, K. G.; Butenas, S.; Brummel, K. *Arterioscler., Thromb., Vasc. Biol.* **2003**, *23* (1), 17−25.
(14) Weiss, E. J.; Hamilton, J. R.; Lease, K. E.; Coughlin, S. R. *Blood* **2002**, *100* (9), 3240−4.
(15) Smyth, S. S.; Reis, E. D.; Väänänen, H.; Zhang, W.; Coller, B. S. *Blood* **2001**, *98* (4), 1055−62.
(16) (a) Pelzer, H.; Schwarz, A.; Heimburger, N. *Thromb. Haemostasis* **1988**, *59* (1), 101−6. (b) Pelzer, H.; Schwarz, A.; Stüber, W. *Thromb Haemost* **1991**, *65* (2), 153−9. (c) Lau, H. K.; Rosenberg, R. D. *J. Biol. Chem.* **1980**, *255* (12), 5885−93.
(17) Olson, E. S.; Whitney, M. A.; Friedman, B.; Aguilera, T. A.; Crisp, J. L.; Baik, F. M.; Jiang, T.; Baird, S. M.; Tsimikas, S.; Tsien, R. Y.; Nguyen, Q. T. *Integr Biol.* **2012**, *4* (6), 595−605.
(18) Josephson, L.; Rudin, M. *J. Nucl. Med.* **2013**, *54* (3), 329−32.
(19) Vogel, J. S.; Love, A. H. *Methods Enzymol.* **2005**, *402*, 402−22. Yamane, N.; Tozuka, Z.; Sugiyama, Y.; Tanimoto, T.; Yamazaki, A.; Kumagai, Y. *J. Chromatogr., B: Anal. Technol. Biomed. Life Sci.* **2007**, *858* (1−2), 118−28.
(20) Sharma, V.; McNeill, J. H. *Br. J. Pharmacol.* **2009**, *157* (6), 907−21.
(21) Prescott, L. F.; McAuslane, J. A.; Freestone, S. *Eur. J. Clin. Pharmacol.* **1991**, *40* (6), 619−24.

SUPPORTING INFORMATION

Disease Detection by Ultrasensitive Quantification of Microdosed Synthetic Urinary Biomarkers

Andrew D. Warren,[†,‡] Shonda T. Gaylord,[§,‡] Kevin C. Ngan,[§] Milena Dumont Milutinovic,[§] Gabriel A. Kwong,[†] Sangeeta N. Bhatia,[†,∥,*] and David R. Walt[§,*]

[†]Harvard-MIT Division of Health Sciences and Technology, Massachusetts Institute of Technology, 77 Massachusetts Avenue, Building 76-453, Cambridge, Massachusetts 02139, United States

[§]Department of Chemistry, Tufts University, 62 Talbot Avenue, Medford, Massachusetts 02155, United States

[∥]Institute for Medical Engineering & Science at MIT, Department of Electrical Engineering & Computer Science, David H. Koch Institute at MIT, and the Howard Hughes Medical Institute, 77 Massachusetts Avenue, Building 76-453, Cambridge, Massachusetts 02139, United States. Division of Medicine, Brigham and Women's Hospital, Boston, Massachusetts 02155, United States.

Text S1

Reporter/peptide synthesis. Thrombin-sensitive reporter 1 (R1) was synthesized by CPC Scientific, with the sequence Biotin-PEG_{5kDa}-Lys(5FAM)-Gly-Gly-DPhe-Pro-Arg-Ser-Gly-Gly-Gly-Cys, where PEG_{5kDa} is 5 kDa poly(ethylene glycol). Biotin-PEG_{5kDa}-Lys(5FAM) serves as a ligand-encoded reporter (R1) that is released upon proteolytic cleavage of the peptide substrate. Standard (non-protease-sensitive) ligand-encoded reporters R1-2 were synthesized by derivatizing biotin-poly(ethylene glycol) 5 kDa-amine (Laysan) with NHS-fluorescein (R1; Sigma) or NHS-Alexa Fluor 488 (R2; Invitrogen) and were purified by illustra NAP-25 Sephadex columns (GE Healthcare). Reporters were quantified by extinction coefficient (Molecular Devices SpectraMAX Plus).

Protease-sensitive R1-NW synthesis. Dextran-crosslinked nanoworms (NWs) were synthesized as previously described.[1] Briefly, NWs were formed by the reaction of Fe(III) chloride hexahydrate and Fe(II) chloride tetrahydrate (both Sigma) with dextran (M_r 15-25 kDa; Fluka) and were aminated by treatment with ammonia. Mean hydrodynamic size by dynamic light scattering (Malvern Instruments Nano ZS90) was 60 nm.

Aminated NWs (approximately 115 kDa each) were activated with N-succinimidyl iodoacetate (SIA; Pierce) in a 1:500 (NW:SIA) molar excess for 1 hour in 50 mM borate, 5 mM ethylenediaminetetraacetic acid (EDTA) buffer, pH 8.3. Activated NWs were purified from excess SIA by fast protein liquid chromatography (FPLC; GE Healthcare) and reacted at a 1:95:20 (NW:peptide:mPEG_{20kDa}-SH) ratio with sulfhydryl-terminated protease-sensitive peptide reporters (thrombin-sensitive R1 is terminated with a cysteine) and mPEG_{20kDa}-SH (Laysan) for 1 hour in the same buffer. Remaining free succinimidyl groups were quenched by the addition of cysteine (Sigma) and protease-sensitive R1-NWs were purified by FPLC into 1x phosphate buffered saline (PBS; Thermo Scientific). Protease-sensitive peptide valency on NWs was quantified by extinction coefficient (Molecular Devices SpectraMAX Plus) as 50-70 per NW. R1-NW concentrations refer to the concentration of thrombin-sensitive R1-substrate peptides on the surface of NWs.

Single molecule array (SiMoA) assay

Preparation of magnetic beads coated with capture antibody. Carboxylic acid functionalized paramagnetic beads (2.7-µm in diameter; Agilent Technologies) were covalently coupled with capture antibody (same as for ELISA) using an in-house 1-ethyl-3-(3-(dimethylamino)propyl)carbodiimide hydrochloride (EDC; Thermo Scientific) coupling protocol. Briefly, beads (100 µL) were washed prior to antibody addition with PBS containing 1%

Tween 20 (Sigma) (wash buffer) and 2-(N-morpholino)ethanesulfonic acid (MES; Thermo Scientific) buffer.

100 µg of either αR1 or αR2 were incubated with beads for 15 min. 1 mL of MES buffer and 100 µL of EDC (10

mg/mL) were added to the bead-antibody solution and incubated for an additional 30 min. After incubation, S2

beads were washed with 1200 µL of wash buffer. A second 40 minute incubation with PBS containing 1% wt/vol BSA was performed to cap any remaining active surface groups. The beads were then washed three times with wash buffer and stored in 200 µL of bead storage buffer.

Formation of reporter-enzyme complex on beads. Serial dilutions of target nanoworms or clearance marker were prepared in 1% urine solutions to generate standard curves. Experimental and control urine containing cleaved nanoworms and clearance marker were diluted 100x in PBS buffer containing 25% FBS (blocking buffer). Each sample was incubated for 2 h in the presence of approximately 200,000 beads. Beads were washed six times with 7.5x PBS containing 0.1% Tween 20 (wash buffer). The bead-protein complex was then incubated with 20 pM of streptavidin-β-galactosidase (SβG; Quanterix) for 30 minutes. Beads were then washed 12 times with wash buffer, once with sucrose buffer and re-suspended in 10 µL of sucrose buffer for loading onto the fiber optic arrays (SCHOTT North America) containing ~50,000 46-fL reaction wells.[2] Cross reactivity experiments were performed as detailed above with 1% vol/vol urine in blocking buffer in the presence of non-target analyte (αR1 beads with R2 or αR2 beads with R1).

Preparation of fiber optic arrays for imaging. Preparation of fiber optic arrays has been previously described.[2] Briefly, optical fiber bundles were polished using 3- and 1-µm diamond lapping films (Allied High Tech Products). To generate wells 4.5 µm in diameter and ~3.25 µm in depth, fibers were etched with 0.025 M hydrochloric acid for 130 seconds, sonicated in water for 10 seconds and dipped in ethanol. To contain beads during loading, etched fibers were wrapped with PVC tubing. Fibers were then loaded with 10 µL of beads and centrifuged at 10,000 x g for 5 min to trap individual beads into wells. Imaging and analysis using a custom-built imaging system has been previously described using fluorescent substrate resorufin-β-D-galactopyranoside (RDG; Life Technologies) and a custom imaging apparatus.[2, 3]

Concentration determination for nanoworm and clearance marker in mice. Urine samples from control or thrombosis-induced mice were diluted 1:10^2 in blocking buffer resulting in a 1% vol/vol urine solution. Capture of R1 and R2 was performed as described above. The equation generated from the linear regression from the standard curves was used to extrapolate the concentration of R1 and R2 present in each sample. Each value was multiplied by 100 to determine the total concentration.

Inulin and R3 plasma and renal kinetics. To compare renal clearance of our reporters to the clinical standard for GFR measurement (fractionated inulin, a 5-10 kDa polysaccharide), we redesigned a third reporter (R3; PEG_{5kDa}-VT750) that is kinetically similar to R1-2, unaffected by proteases, and may be detected from plasma by near-infrared fluorescence. Inulin (10 mg/kg; BioPAL) and R3 (5 µM) were coinjected into female Swiss

Webster mice (n=7) and plasma concentration of each was quantified at approximately 5 min intervals for 60 min. At 60 min, urine was collected. Inulin was quantified by competitive inulin ELISA (BioPAL) and R3 was quantified by near-infrared fluorescence (LI-COR Odyssey). Plasma half-life was calculated using a single exponential decay fit on all lumped data points and renal concentration factor was calculated as urine concentration normalized to peak plasma concentration. Statistical tests were paired Student's *t* test.

Thromboplastin-induced model of venous thrombosis. Thrombin-sensitive R1-NWs and renal clearance control R2 were IV coinjected in equimolar amounts at 0.2-200 pmol in 200 µL PBS into female Swiss Webster mice (n=5-10 per concentration) and all urine 0-30 min post-injection was collected to obtain control clearance values. 3-5 days later (to allow synthetic biomarker clearance), mice were again coinjected with R1-NWs and R2 along with 20 U/g body weight thromboplastin (Biopharm Laboratories) to induce intravascular coagulation as previously described[4] and all urine 0-30 min post-injection was collected. R1 and R2 concentrations were quantified by ELISA (20-200 pmol) or SiMoA (0.2-2 pmol). This model of pulmonary embolism initiated by the extrinsic clotting cascade has been characterized in the hematology literature by our group and others to produce a rapid formation of blood clots that embolize to the lungs to recapitulate this life-threatening condition.[4] This model has been used to characterize the roles played by different vascular receptors in thrombosis development and to understand the function of new antithrombotic agents. To ensure accurate use of this model, we have used injected doses of thromboplastin similar to these studies and consequently expect similar physiological levels of clotting.

Mouse-human scaling and microdose calculations.

Microdosing calculations. Though interspecies protease kinetics are similar, blood volume and renal clearance differences should be considered to obtain a reasonable microdose estimate. Blood volume varies approximately linearly with weight;[5] an average 62 kg human[6] therefore has approximately 2200 times the blood volume of the average 28 g mouse used in this study. Our synthetic biomarker injection has an adjusted molecular weight of 19.7 kDa (see below for calculations). Adjusting for blood volume, a 100 µg microdose in humans is approximately 2.3 pmol for mice (100 µg / 19.7 kDa / 2200 blood volume difference). Therefore, our synthetic biomarker doses of 0.2-2 pmol are beneath the approximate microdose threshold for humans. Here, consideration of renal clearance differences (~16x slower GFR in humans as quantified by inulinn clearance[7]) is neglected: decreased rate of reporter reporter clearance results in a less than 4x difference in urine concentration after 30 min, which may be easily resolved by the SiMoA assay sensitivity. Minor interspecies

variation in clotting cascade regulation and function are also ignored, as key hemostatic coagulation metrics are very similar between mouse and human (Table S1).

Molecular weight calculations. The nanoworms used in these studies have an average molecular weight of 115 kDa. During synthesis, nanoworms were reacted with a 20-fold excess of 20 kDa PEG-SH (total MW 400 kDa), and average valency of 6.6 kDa peptide-reporter per nanoworm was measured to be approximately 70. Therefore, the total molecular weight of a thrombin-responsive R1-NW was approximately 975 kDa (115 + 20*20 + 6.6*70). As we considered concentration by functional substrate available, this is an effective molecular weight of ~14 kDa per peptide-reporter. Adding the molecular weight contribution of free R2 (approximately 5.8 kDa), the adjusted molecular weight per reporter is 19.7 kDa.

Supplementary Figures

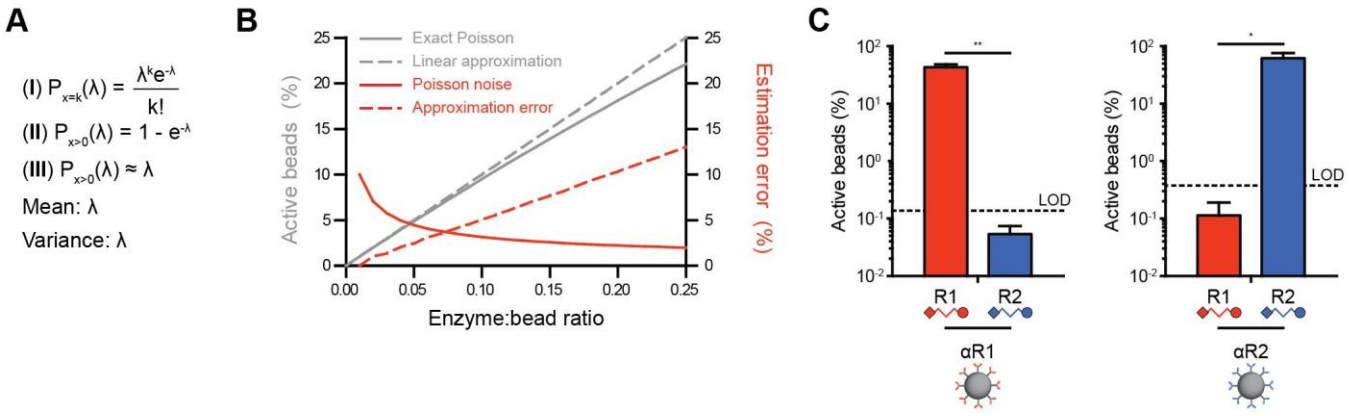

Figure S1. (A) The Poisson probability distribution function (I) describes the frequency at which *x* events occur with an average of λ. In our digital ELISA system, we determine the probability of a particular well being "on" – that is, having one or more active enzymes. For all λ (ratio of enzymes to beads), this may be expressed as (II). A first order Taylor series approximation of (II) around λ=0 demonstrates that the probability of a bead being active is linear with the enzyme:bead ratio (III) for small λ. (B) Our SiMoA assay enables concentration quantification by counting the proportion of rare events. Even with perfect reporter capture efficiency, assay sensitivity is limited by Poisson noise ("shot noise" due to distribution variance $\sigma^2=\lambda$) more than approximation error. (C) Assay specificity was quantified using saturating concentrations of R1 and R2 on either αR1 (*Left*; *P*=0.0051) or αR2 (*Right*; *P*=0.018) capture beads. Here, capture efficiency of non-cognate reporters (e.g., R1 by αR2) was below the limit of detection (LOD; defined as $\mu_{BG}+3\sigma_{BG}$) of each assay.

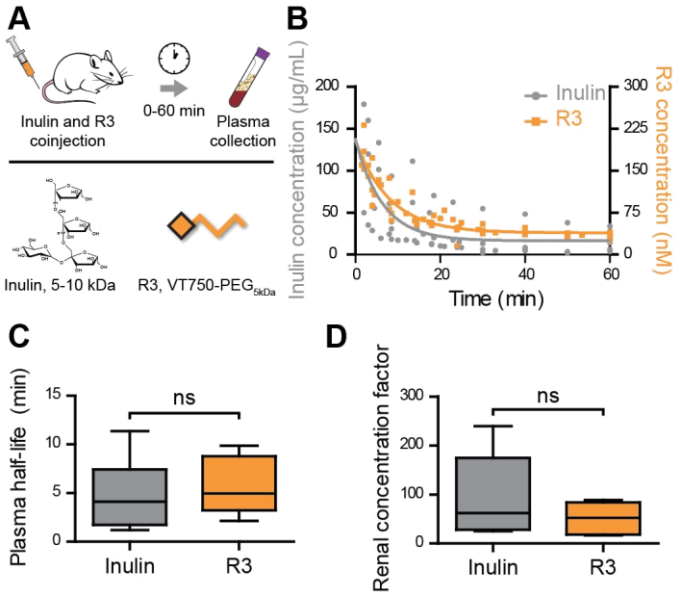

Figure S2. (A) Inulin is a 5-10 kDa polysaccharide used in the clinic to assess glomerular filtration rate (GFR) as it is small, stable, and not actively handled by the nephron. To compare pharmacokinetics of our reporters to inulin, we coinjected inulin and a near-infrared fluorescent derivative of our reporters (R3; VivoTag750-PEG_{5kDa}) in female Swiss Webster mice and observed plasma kinetics and renal handling. (B) Analysis of plasma concentration of inulin and R3 over the course of 1 hour (n=7; timepoints taken approximately every 5 min) demonstrated a first-order decay process. (C) Blood half-lives for both compounds using these same data points were statistically indistinguishable (P=0.57). (D) Renal concentration factor (urine concentration after 1h normalized to peak plasma concentration) was also not significantly different between gold standard inulin and our reporter R3, suggesting rapid renal clearance and a lack of active handling by the nephron (P=0.17). Statistical tests were paired Student's t test.

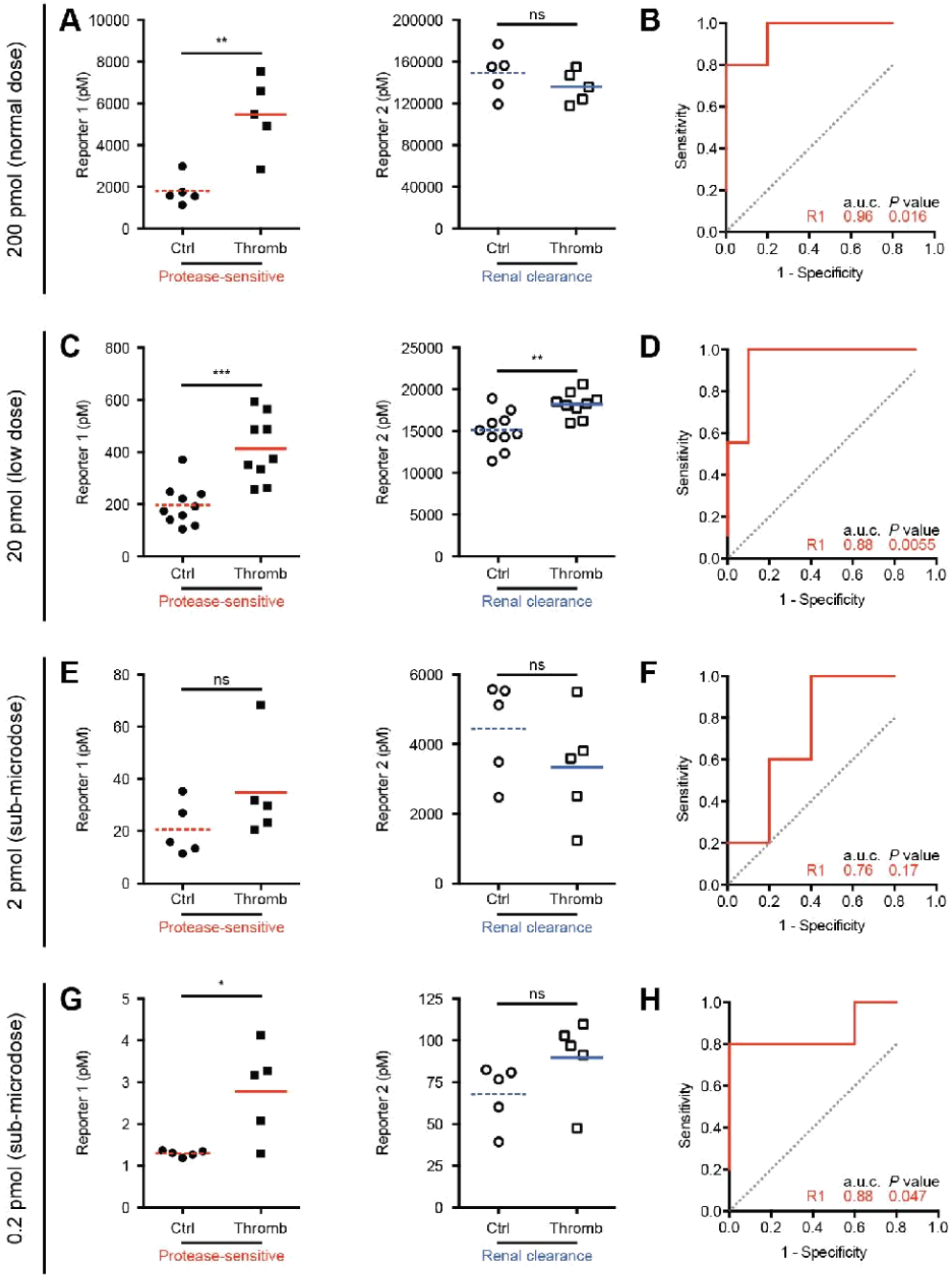

Figure S3. 0.2-200 pmol thrombin-sensitive NW-R1 and renal clearance control R2 were coinjected in female Swiss Webster mice (n=5-10) with either thromboplastin (to induce intravascular coagulation) or PBS. (A,C,E,G) At 200, 20, and 0.2 pmol injected doses, disease resulted in higher renal clearance of thrombin-sensitive R1 as detected by ELISA or SiMoA (*Left*; *P* values are 0.0027, 0.0003, 0.1837, 0.017 from high to low injected dose), while R2 remained relatively constant with fold changes between groups of 0.75-1.32 (*Right*; *P*

values are 0.30, 0.0025, 0.27, 0.15 from high to low injected dose). (B,D,F,H) Receiver-operating characteristic (ROC) curves for each injected dose indicate the diagnostic ability of R1 concentration in urine.

Hemostatic coagulation index	**Human**[8] (healthy clinical range)	**Male Swiss Webster mice**[9] (mean ± SD)	**Female CD-1 mice**[10] (mean ± SEM)	**Female CD-1 mice**[11] (interquartile range)
Prothrombin time (PT; s)	11.5 – 13.5	10.2 ± 1.0	11.9 ± 0.30	14.0 – 14.6
International normalized ratio (INR; unitless)	0.8 – 1.4	0.88 ± 0.09	Not given	Not given
Activated partial thromboplastin time (aPTT; s)	27 – 38	19.4 ± 1.4	22.5 ± 0.60	33.1 – 37.2
Thrombin time (TT; s)	10 – 14	16.6 ± 1.5	12.8 ± 0.40	22.0 – 25.5
Fibrinogen (mg/dL)	123 – 370	266 ± 54	188 ± 6.4	Not given

Table S1. Overview of standard values for five hemostatic coagulation indices regularly used in the clinic. Overall, the clotting cascade is highly conserved between mice and humans in terms of both sequence homology and functional clotting characteristics. Our pulmonary embolism model uses thromboplastin to trigger the extrinsic clotting cascade via the complexation of factor VII and tissue factor; consequently, prothrombin time (PT; a measure of extrinsic clotting cascade function) is the most relevant parameter to consider between organisms. A survey of three studies that quantify PT in healthy mice report values similar to those expected in healthy humans, indicating no large interspecies differences in relevant measures of clotting function.[8-11]

References

1. Park, J. H.; von Maltzahn, G.; Zhang, L.; Schwartz, M. P.; Ruoslahti, E.; Bhatia, S. N.; Sailor, M. J., *Adv Mater* **2008,** *20* (9), 1630-1635; Park, J. H.; von Maltzahn, G.; Zhang, L.; Derfus, A. M.; Simberg, D.; Harris, T. J.; Ruoslahti, E.; Bhatia, S. N.; Sailor, M. J., *Small* **2009,** *5* (6), 694-700.
2. Rissin, D. M.; Kan, C. W.; Campbell, T. G.; Howes, S. C.; Fournier, D. R.; Song, L.; Piech, T.; Patel, P. P.; Chang, L.; Rivnak, A. J.; Ferrell, E. P.; Randall, J. D.; Provuncher, G. K.; Walt, D. R.; Duffy, D. C., *Nat Biotechnol* **2010,** *28* (6), 595-9.
3. Rissin, D. M.; Fournier, D. R.; Piech, T.; Kan, C. W.; Campbell, T. G.; Song, L.; Chang, L.; Rivnak, A. J.; Patel, P. P.; Provuncher, G. K.; Ferrell, E. P.; Howes, S. C.; Pink, B. A.; Minnehan, K. A.; Wilson, D. H.; Duffy, D. C., *Anal Chem* **2011,** *83* (6), 2279-85.
4. Lin, K. Y.; Kwong, G. A.; Warren, A. D.; Wood, D. K.; Bhatia, S. N., *ACS Nano* **2013,** *7* (10), 9001-9; Smyth, S. S.; Reis, E. D.; Väänänen, H.; Zhang, W.; Coller, B. S., *Blood* **2001,** *98* (4), 1055-62; Weiss, E. J.; Hamilton, J. R.; Lease, K. E.; Coughlin, S. R., *Blood* **2002,** *100* (9), 3240-4.
5. Sharma, V.; McNeill, J. H., *Br J Pharmacol* **2009,** *157* (6), 907-21.
6. Walpole, S. C.; Prieto-Merino, D.; Edwards, P.; Cleland, J.; Stevens, G.; Roberts, I., *BMC Public Health* **2012,** *12*, 439.
7. Prescott, L. F.; McAuslane, J. A.; Freestone, S., *Eur J Clin Pharmacol* **1991,** *40* (6), 619-24.
8. Gomella, L.; Haist, S., *Clinician's Pocket Reference*. 11 ed.; McGraw-Hill Medical: 2006.
9. Liu, J. Y.; Li, N.; Yang, J.; Qiu, H.; Ai, D.; Chiamvimonvat, N.; Zhu, Y.; Hammock, B. D., *Proc Natl Acad Sci U S A* **2010,** *107* (39), 17017-22.
10. Lemini, C.; Jaimez, R.; Franco, Y., *Thromb Res* **2007,** *120* (3), 415-9.
11. Palm, M.; Frankenberg, L.; Johansson, M.; Jalkesten, E., *Comparative Haematology International* **1997,** *7* (4), 243-246.